Use of the Geomaterial for the Elimination of Surfactant Dodecylbenzene Sulfonic Acid from Aqueous Solution

G. Mimanne [1], R. Sennour [1], A. Benghalem [1*], S. Taleb [1], K. Benhabib [2]

[1]Laboratory of materials & catalysis, Department of chemistry, Faculty of sciences,
University Djillali Liabes B.P 89, 22000, Sidi Bel Abbes, Algeria.
[2]Eco-Procédés, Optimisation et Aide à la Décision (EPROAD, JE), University of Picardie Jules Verne, IUT of Aisne, 48
street of Ostende, 02100, Saint-Quentin, France

Abstract

This study is dealing with the removal of dodecylbenzene sulfonic acid surfactant (DBSA) by a new geomaterial composite formed by bentonite (mostly Ca-montmorillonite) and activated carbon. Both components are the sorbent which are bonded with concrete. The DBSA surfactant enters the environment primarily through wastewater and sludge; this can lead to severe water resource pollution. A series of batch adsorption experiment were carried out under various operating; initial concentration, pH, temperature, concentration dose of the adsorbent and the surfactant. The interest of this study lies whether the new material has more promising sorbent properties than the individual components. A comparison between the geomaterial and its individual components has been established by performing adsorption and kinetic experiments. The results indicate that the removal of DBSA was primarily attributed to the potential sorbent of the inorganic part of geomaterial. The critical micelle concentration (CMC) was found to play an important role because there was no further adsorption beyond the CMC value. Equilibrium isotherms were analyzed by Langmuir, Freundlich, Temkin and Dubinin-Radushkevich (D-R) equations. The equilibrium data were well described by Langmuir and D-R equations at all range of operating parameters.

Keywords: Geomaterial, Surfactant, Dodecylbenzene sulfonic Acid, Adsorption, Critical Micelle Concentration.

1. Introduction

The Dodecylbenzene sulfonic acid derived from linear alkyl benzene sulfonate (LAS) series is extensively applied anionic surfactant. It is a raw material for detergent mainly used to produce household detergents including an emulsifier for agricultural herbicides. LAS are used in large quantities and enter the environment primarily through wastewater and sludge [1]. The extensive applications of surfactants have produced environmental pollution and have raised problems in wastewater treatment plants [2]. The experimental data have shown that surfactants can kill micro-organisms at very low concentrations (1-5 mg.L^{-1}) and harm them at even lower concentrations (0.5mg.L^{-1}) [3]. In addition, surfactants can produce foams which are a significant problem in sewage treatment. Therefore, the removal of the surfactants from wastewater is important in reducing their environmental impact. Many techniques have been used for the removal of surfactants in aqueous solution. Among these, biological degradation, ozonation and extraction are often costly with may possibly create secondary pollution because of excessive use of chemicals [4-5-6]. In addition, a large number of surfactants used at present, like linear alkylbenzene sulphonates that have relatively low biodegradability [7]. The adsorption process seems to be an effective method for the removal of surfactants, especially in the case of low concentrations of surfactant. A number of adsorption systems have been explored for the removal of

surfactants [8]. Numerous adsorbents, such as activated carbon, layered double hydroxides, silica, mineral oxides and natural biomasses, have been extensively investigated [9-10-11] . Recently research has focused on low cost and easily available materials such as waste activated carbon and rubber granules [12]. It was found that geomaterial made from inorganic and organic component was able to effectively adsorb some VOCs from wastewater due to its particular structure [13]. This kind of material has a high content of functional groups that could bind with the hydrophobic and hydrophilic parts of surfactants by electrostatic forces or hydrophobic bonds [14]. Therefore geomaterial has the potential to be used as a low-cost adsorbent for the removal of surfactants from wastewater. The purpose of this study was to investigate the adsorption behavior of one geomaterial towards the surfactant DBSA. The objective was to evaluate the DBSA removal potential and related kinetics of geomaterial due to the fact that it is abundant and an inexpensive material compared to activated carbon [13]. The geomaterial composite is formed by bentonite (mostly Ca-montmorillonite) and activated carbon. Both components are the sorbent which are bonded with concrete. Equilibrium adsorption experiments were carried out with the anionic surfactant DBSA which is most frequently used in detergent. The surfactant concentrations used are lower than their critical micelle concentrations CMCs and higher than that found in the wastewater. The research papers reports the application of various two-parameters adsorption isotherms Langmuir, Freundlich, Temkin and D-R based on the statistical judgment obtained from a series of linear and non linear function errors analysis.

2. Experimental details

2.1. Chemicals
Dodecylbenzene Sulfonic Acid solution of linear Formula $C_{12}H_{25} C_6H_4SO_3H$, with purity > 95%, is purchased from Aldrich GMBH (Schnelldorf, Germany), is used without further purification. The chain length of DBSA is C_{12}-C_{18} (equally distributed, average molecular weight of DBSA is 326.49 g.mol^{-1}). The DBSA surfactant is brown viscous liquid, it is hygroscopic (absorbs moisture from the air), stable under normal temperatures and pressures and it is soluble in water.

2.2 Preparation of adsorbent
The geomaterial was prepared by assembly of several constituents: montmorillonite rich bentonite (80%), Cement (2%) and activated carbon (18%). These materials were chosen in order to associate the mechanical solidity due to the cement and the adsorptive properties due to the active carbon and the clay mineral. Before mixture, the montmorillonite underwent a treatment of purification by sedimentation, followed by chemical treatment [15]. The product was then saturated with calcium ion by stirring in a 1M calcium chloride solution and used as such, it was noted Ca^{2+}-MM. The amounts of activated carbon AC of very fine powder (particles size lower than 0.2 μm) and cement were mixed then dispersed in a solution of 50 mL Ca^{2+}-MM. The mixture was stirred for 24 hours and dried at room temperature then grounded into granular with diameter of particles < 0.2 μm. The final product obtained is called a geomaterial, it was noted *GeoM*. The chemical composition and physical properties of materials are given in (Table 1).

Table 1: Characterization of adsorbents

Adsorbent	Raw Material	Activation method	BET surface Area (m^2.g^{-1})	Pore Volume (cm^3.g^{-1}) at P/P$_0$= 0,99	Average Pore size (nm)	Supplier
AC	wood	H$_3$PO$_4$	1423	1,06	3,0	Norit*
Ca^{2+}-MM	MM	H$_2$O$_2$/HCl	81	0,09	4,7	ENOF**
GeoM	Ca^{2+}-MM, AC,Cement	-	170	0,52	9,3	LMC***

*: Powder Activated carbon.

**: National Company for Nonferrous Mining Products and useful substances

***: Laboratory of Materials & Catalysis

2.3 Characterization methods
The specific surface area, pore and pore volume distribution were measured using the Micrometric Tristar 3000 surface area and porosimetry analyzer. The samples were pre-treated overnight to remove water and other contaminants from the pores. During the pretreatment, a nitrogen flow was applied and the samples were heated to 150°C for 24 hours. The measured physical properties are listed in (Table 1).

2.4 Adsorption experiment
Adsorption tests were carried out in a batch process by varying adsorbent amount, initial concentration of DBSA (5.6 to 30 mM.L^{-1}) at pH = 4. The amounts of GeoM were dispersed in 50mL DBSA solution and placed in a shaking bath (Julabo SW22) at 25 °C. To be absolutely certain that equilibrium was reached, 48 hours equilibrium time was used in all further experiments. After equilibration, the dispersions were filtered through a 0.2 µm and analyzed. All experiments were conducted in duplicate. The equilibrium concentration of DBSA was determined by spectrophotometrically (UV–Vis Spectrometer Lambder, type 2401 PC fitted with a UV–Visible detectors set) at λ_{max}=268 nm. The effects of temperature, pH value and adsorbent dose on the adsorption capacity of the adsorbent to DBSA were also investigated. We used 0.1N of HCl or 0.1N of NaOH in order to adjust the pH value of solutions.

The adsorption capacity of surfactant on the adsorbent, q_e (mg.g^{-1}) was calculated by mass balance relation (1):

$$q_e = \frac{(C_i - C_e)}{m} V \qquad\qquad (1)$$

where m, V, C_i and C_e are the mass of the adsorbent (g), the volume of the solution (L), the initial concentration of the DBSA solution and equilibrium concentrations (mol.L^{-1}) respectively.

2.5 Determination of critical micelle concentration of DBSA surfactant Procedure
A surfactant solution of the higher concentration (50 mM.L^{-1}) was prepared. To measure the specific conductivity of the DBSA surfactant we followed the step-by-step dilution–extraction method [16]. The conductivity measurements were carried out in a jacketed beaker thermostated at 25°C by circulating water and by using a knick microprocessor conductimeter provided with a four-pole measuring cell (factor cell 1.1 cm^{-1}). Micelles are small colloidal particles, relative to the wavelength of light. When micelles form, the aqueous surfactant solution behaves as a microheterogeneous medium. The value of the CMC can be determined by the change in the physicochemical properties of the surfactant solution as the surfactant concentration increases. Experimentally, the CMC is found by plotting a graph of a suitable physical property as a function of surfactant concentration. An abrupt change of slop marks the CMC.

3. Results and discussion
3.1. Effect of initial DBSA concentration
Several adsorption experiments showed that an equilibration time of 6 hours for GeoM was sufficient to achieve steady state, since till 10 hours, C_e change slightly. The kinetic of DBSA adsorption at various initial concentrations are presented in (Figure 1). At low initial concentrations, the adsorption equilibrium was quickly reached and saturation was achieved, while with high initial concentrations the adsorption was slow and saturation was not reached due to uncompleted reaction**.**

3.2. Effect of adsorbent quantity
The results indicate that 2g of AC and 3g of Ca^{2+}–MM are required to remove 90% and 70% of DBSA surfactant**,** while a small quantity of GeoM 0.3 g is sufficient to remove 83% of DBSA (Table 2). The extent of removal of DBSA could not be further increased when the offer of adsorbent exceeded these values. This might be due to the particle interaction, such as aggregation resulting from high adsorbent concentration (figure 2) [17]. Such aggregation would lead to a decrease in the total surface area of adsorbent and an increase in diffused path length [17].
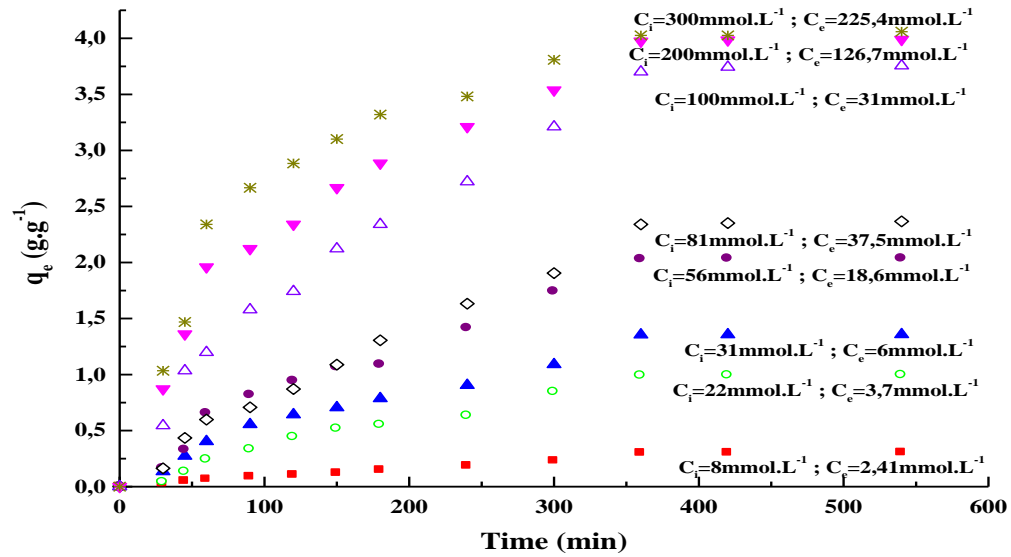
Figure 1. Effect of initial DBSA concentration on GeoM, μ = 500 rpm, m = 0.3g, pH = 4.5, T= 25°C.

Table 2: Effect of weight of adsorbents

Adsorbents	GeoM	AC	Ca^{2+}-MM
Amount of adsorbent (g)	0,3	2	3
Extent of DBSA removal (%)	82,86	89,4	70,31
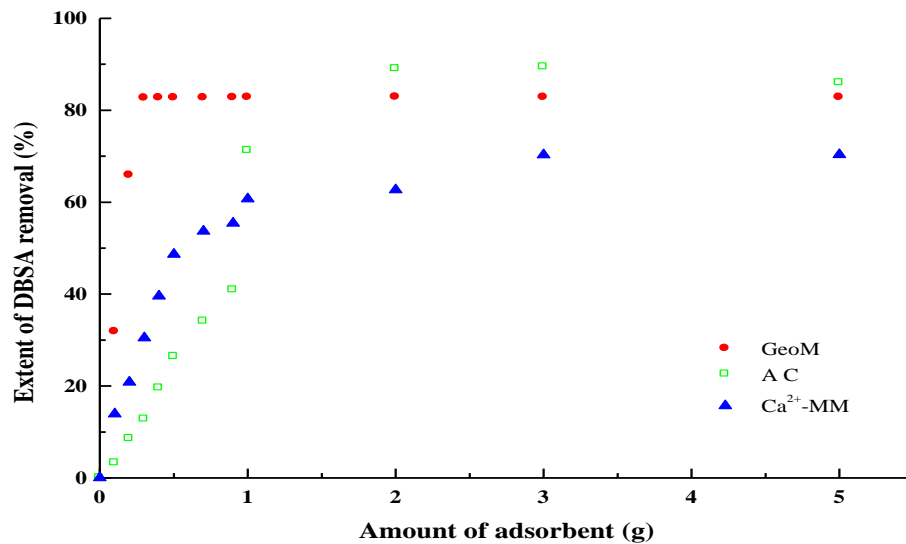
Figure 2. Effect of adsorbent quantity, μ = 500 rpm, C_i = 2.2 mMol.L^{-1}, pH = 4.5, T= 25°C.

3.3. Effect of pH

The acidity or/and the basicity affect considerably the elimination of DBSA [18] as shown in figure 3. The GeoM exhibits high adsorption efficiency for DBSA with removal higher than 83% within a pH range of 2.0-

J. Mater. Environ. Sci. 3 (4) (2012) 712-725
ISSN : 2028-2508
CODEN: JMESCN

Mimanne et al.

4.0, the extent of removal decreased dramatically at pH>6.0. Adsorption at lower pH could be attributed to the inorganic part of the GeoM, the surface will then exhibit an anion exchange capacity favorable to anionic DBS⁻. The decrease in adsorption of DBSA observed at alkaline pH is probably due to the neutralization with the acid sites on the montmorillonite, and the competition between OH⁻ and anionic surfactant for the adsorption sites [18].
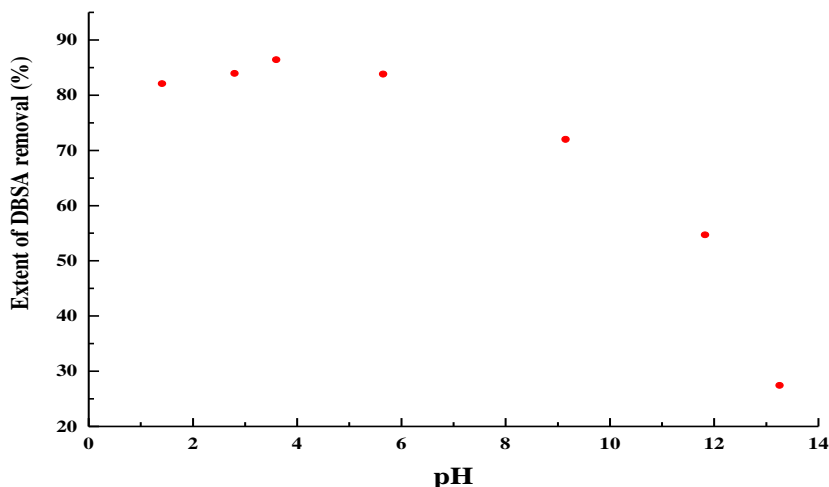
Figure 3. Effect of pH on the adsorption of DBSA on GeoM, µ=500 rpm, C_i=2.2 mMol.L⁻¹, m= 0.3g, T= 25°C.

3.4. Effect of contact time
Three adsorbents with different structures present different kinetic adsorption (Figure **4**). For both AC and Ca²⁺-MM adsorbents the sorption equilibrium is reached after 1-2 hours respectively, while for the GeoM adsorbent, equilibrium is reached after 6 hours only.
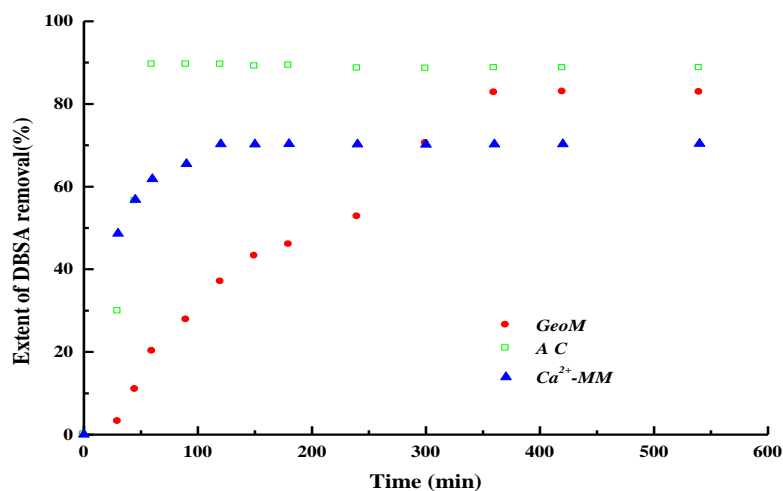
Figure 4. Effect of Contact time on the adsorption of DBSA on different adsorbents, µ=500 rpm, C_i=2.2 mMol.L⁻¹, T= 25°C, pH= 4.5.

Moreover the curving observed in the kinetics of GeoM at 4 hours, suggests that pseudo equilibrium takes place at this instant, with DBSA removal of 66%. Beyond, the adsorption continues during 2 hours reaching the final

equilibrium with removal of 33%. A conclusion can be made the DBSA removal by the composite was occurring in two stages: the first one controlled by the clay and accounting for 66% of DBSA sorption, the other one controlled by the AC and accounting for 33%. This is assumed because of the effect of the following parameters: the heterogeneous texture of the geom constituted by the surfaces of the inorganic clay and of the Activated carbon; these surfaces presenting various sites of adsorption will impose a selective diffusion of the DBSA surfactant through the geom.

3.5. Effect of the CMC value
3.5.1 Measures
The electrical conductivity method can only be applied to measure the CMC of ionic surfactants. The change in the electrical conductance of aqueous ionic surfactant solutions at the CMC is due to the different degree of surfactant ionization below (surfactant monomers behave as strong electrolytes) and above (micelles are partially ionized) the CMC. On the assumption that the aqueous surfactant solutions obey Kohlrausch's law [19], the specific conductivity, k, of surfactant solutions can easily be calculated in terms of the molar ionic conductivities of ions   ($\lambda_i = z_i u_i F$, where z and u are the charge and mobility of the ion, and F the Faraday constant); ionic charges are omitted in the subscripts for the sake of simplicity [20]. Let us consider the case of DBSA under two conditions:

   i)   Below the CMC, it is accepted that no micelles are formed; then the specific conductivity of aqueous DBSA solution, in $mS.cm^{-1}$ ($S=\Omega^{-1}$), is made up of independent contributions of anions $CH_3(CH_2)_{11}–C_6H_6SO_3^-$ DBS^- anions and H^+ cations:

$$K = (\lambda_{H+} + \lambda_{DBS-})[DBSA] = m_1[DBSA] \qquad (2)$$

where m_1 is the slope of the plot of the specific conductivity k versus [DBSA] below the CMC.

   ii) Above the CMC, the conductivity of ionic surfactants such as DBSA usually decreases. This is explained by the inclusion within the micelle of ions of opposite charge (counterions) to the long-chain ions.

3.5.2. Correlation of the CMC value
The adsorption capacity at surfactant concentration of 2.2 $mM.L^{-1}$ is shown in (Figure **5**), since this concentration of DBSA was expected to be at least present in wastewater. This concentration is below the CMC value of DBSA 4.6 $mM.L^{-1}$ and therefore it was assumed that monomer adsorption will take place. At concentrations above 4.6 $mM.L^{-1}$ micelles will exist next to the DBSA monomer. It was expected that at equilibrium concentrations above the CMC, the adsorption capacity will approach a constant value because the free monomer concentration became approximately constant. This can be assumed because the equilibrium between the micelles and monomers was very rapid [21].

    Moreover the isotherm (Figure **5**) shows that adsorption process occurs in two steps depending on the CMC value:
   1. The first step occurred below the 0.66 CMC involving the Ca^{2+}-MM adsorbent,
   2. The second step occurred beyond the 0.66 CMC involving the AC adsorbent.

- Until the 0.66 CMC, the adsorption of DBSA is concerned with Ca^{2+}-MM adsorbent according a pseudo-equilibrium reached with a ratio of 66%. This result is in good agreement with the results of the DBSA removal obtained in the contact time.
- Beyond the 0.66 CMC value, due to the presence of the free uptake of the DBSA monomers, the adsorption took place onto the adsorbent AC, and increased until the equilibrium concentration of 1.0 CMC then remained constant.
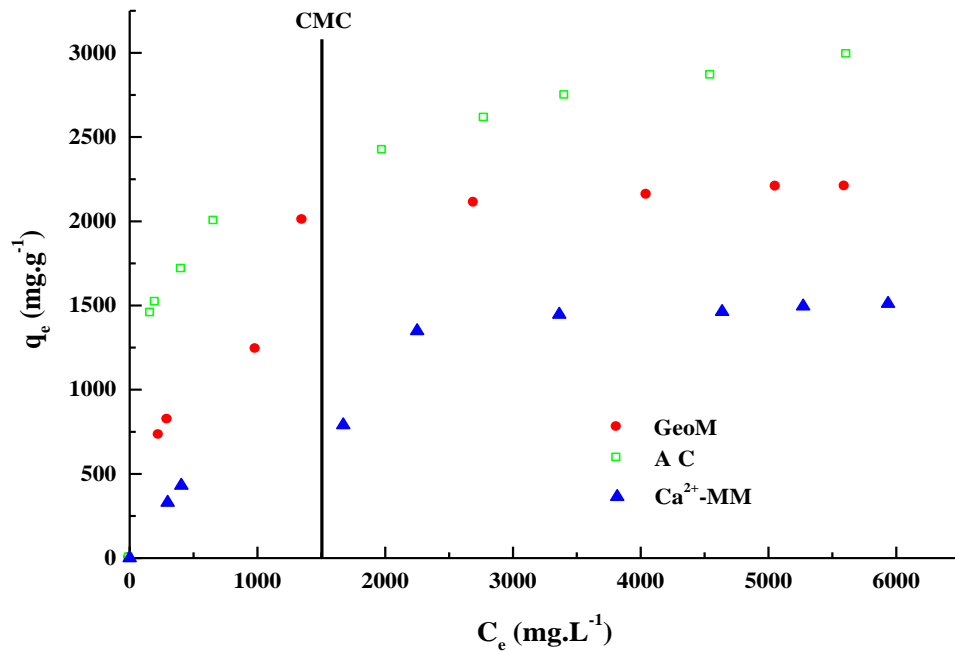
Figure 5. Adsorption isotherms for DBSA-Adsorbents and the CMC effect, μ=500 rpm, C_i=2.2 mMol.L^{-1}, T= 25°C, pH= 4.5.

3.6. Adsorption Isotherms

In order to choose the best isotherm model to represent DBSA–Materials adsorption system, a set of equilibrium data has been tested on the Langmuir [22], Freundlich [23], Temkin [24] and D-R [25] isotherm models, respectively. The model equations are shown below (Equations 3-6):

$$\frac{q_e}{qm} = \frac{K_L C_e}{1 + K_L C_e} \tag{3}$$

$$q_e = K_F C_e^{1/n} \tag{4}$$

$$q_e = \beta \ln K_T C_e \tag{5}$$
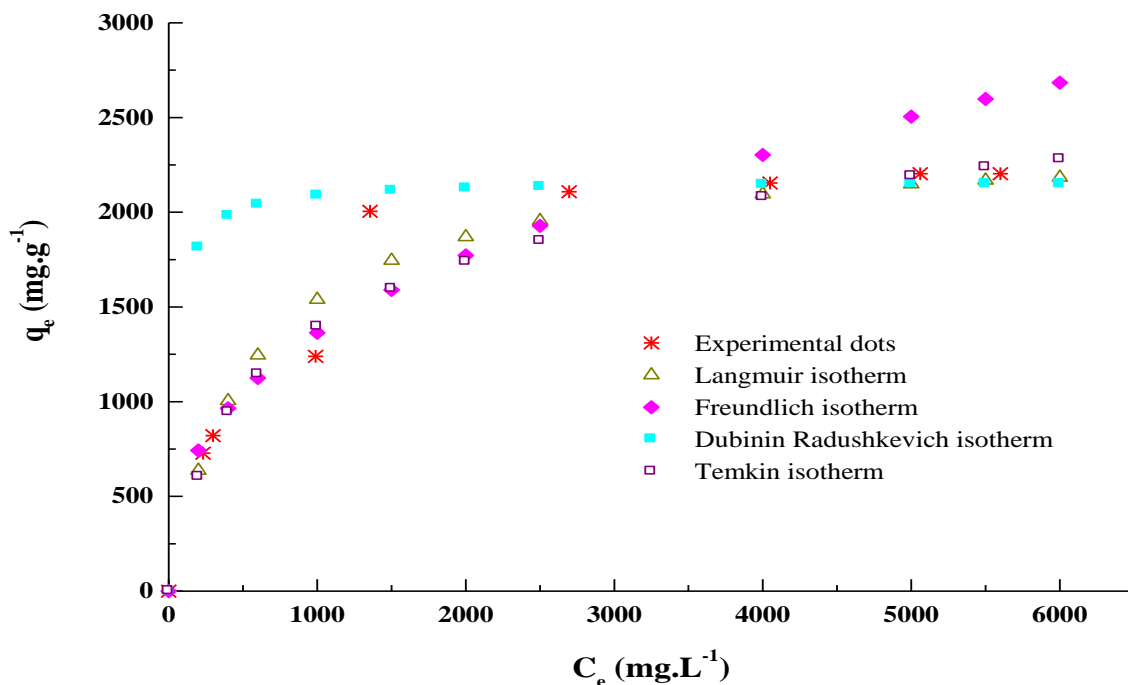
$$q_e = q_s \exp(-K_D \varepsilon^2) \tag{6}$$

where q_e, C_e, K_L and q_m are the adsorption capacity in equilibrium (mg.g^{-1}), the sorbate equilibrium concentration (mg.L^{-1}), the Langmuir constant associated to energy of adsorption (L.mg^{-1}) and the theoretical monolayer adsorption capacity (mg.g^{-1}) respectively.

K_F is the Freundlich constant (mg.g^{-1})·(L.mg^{-1})$^{1/n}$ while 1/n is dimensionless heterogeneity factor. β is the Temkin constant related to heat of adsorption (kJ.mol^{-1}). K_T is the equilibrium binding constant (L.mol^{-1}) corresponding to the maximum binding energy. q_s is the D-R isotherm constant (mg.g^{-1}), ε is the Polanyi potential constant (kJ^2 kmol^{-2}) given as *RTln(1+1/C_e)* with R is the universal gas constant, T is the absolute temperature (K) and KD is related to the free energy of sorption (mol^2.kJ^{-2}). The mean free energy of adsorption E (kJ.mol^{-1}) from D-R equation can be computed using the following relationship: E = 1/√2K$_D$ [26]. Prior to equilibrium data plotting, all model equations were linearized accordingly. The values of the constants for Langmuir, Freundlich, Temkin and D-R isotherm models at 303K for the removal of DBSA onto different adsorbents are presented in (Table 3).

Table 3: Isotherms constants of DBSA-Materials adsorption system.

Model	Constants		GeoM	A C	Ca²⁺-MM
Langmuir	**R²**	**q_m**	0,99	0,95	0,98
	(mg.g⁻¹)	**K_L**	2453	2594,4	1687,65
	(L.mg⁻¹)	**SSE**	$1,74.10^{-3}$	7.10^{-3}	$8,22.10^{-4}$
	%		1,52	0,85	1,52
Freundlich	**R²**	**1/n**	0,92	0,98	0,94
	K_F(mg.g⁻¹)(L.mg⁻¹)¹ᐟⁿ		0,49	0,22	0,60
	SSE %		47,42	458,5	11,01
			5,58	2,89	2,83
Temkin	**R²**	**β**	0,98	0,96	0,98
	(kJ.mol⁻¹)	**K_T**	0,5	0,34	0,41
	(L.mol⁻¹)	**SSE %**	0,02	0,43	0,0075
			2,74	2,12	2,14
D-R	**R²**	**q_s**	0,98	0,93	0,99
	(mg.g⁻¹)	**K_D**	2163,7	2481,9	1471,7
	(mol².j⁻²)	**SSE %**	0,014	0,0035	0,033
			1,92	0,98	1,2

Figure 6, 7 and 8 illustrate the adsorption isotherms of DBSA for the GeoM, Ca²⁺-MM and AC respectively. The theoretical monolayer adsorption capacities are founded to be higher, indicating that the adsorption occurs favorably. The value of 1/n less than 1 describes a favorable nature of DBSA adsorption onto all adsorbents.
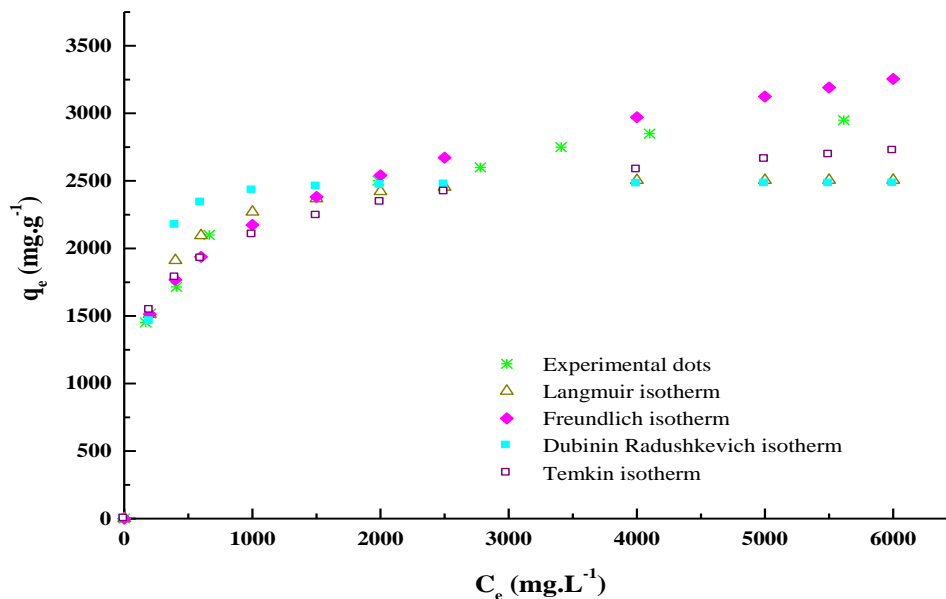

Figure 6. Adsorption isotherm of DBSA onto GeoM, μ=500 rpm, C_i=2.2 mMol.L⁻¹, T= 25°C, pH= 4.5, m= 0.3g

J. Mater. Environ. Sci. 3 (4) (2012) 712-725
*ISSN : 2028-2508*
CODEN: JMESCN

Mimanne et al.

According to table (3), linear regression coefficients of Langmuir isotherm indicates a strong correlation between the experimental data and the model mainly for GeoM and Ca^{2+}-MM material.

However the data seem to be less in agreement with Freundlich except for the AC adsorbent where the R^2 value was 0.98. Further analysis of sum of squared errors (SSE) revealed that both models are applicable since the resulting errors were very small. The findings are very important to indicate that adsorbent might have homogeneous and heterogeneous surface energy distributions. Both energy distributions induce single and multilayer adsorption. These might occur simultaneously or subsequently by order of time (one after another), both in a random manner. A trend in satisfying multiple models is no longer peculiar since many researchers have reported the similar findings [27].

Figure 7. Adsorption isotherm of DBSA onto AC, μ=500 rpm, C_i=2.2 mMol.L^{-1}, T= 25°C, pH= 4.5, m= 2g.
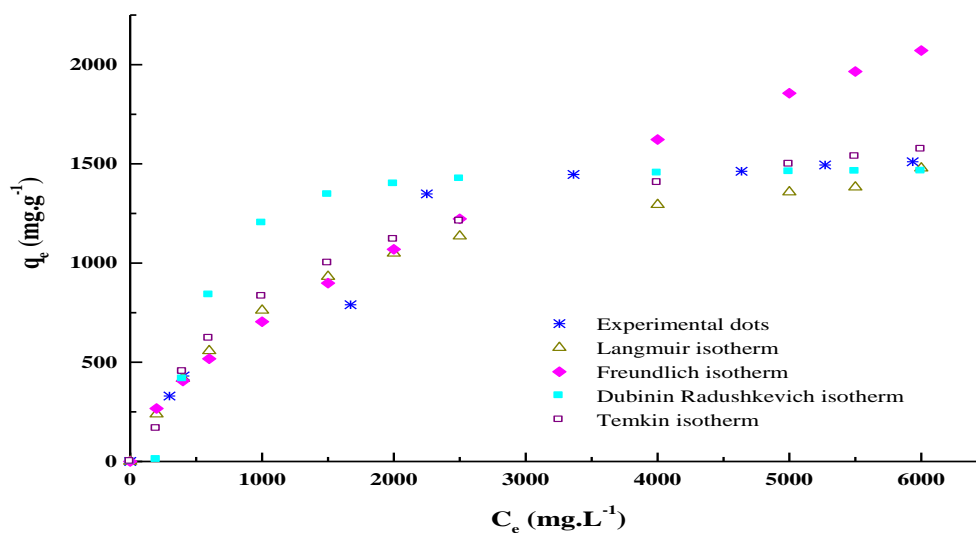
Figure 8. Adsorption isotherm of DBSA onto Ca^{2+}-MM, μ=500 rpm, C_i=2.2 mmol.L^{-1}, T= 25°C, pH=4.5, m=3g

According to the Temkin isotherm, the β values associated to the heat of the DBSA adsorption onto the adsorbents ranging from 0.34 to 0.50 kJ.mol^{-1}. This is a sign of a low interaction between DBSA molecules and the adsorbents surface. The Temkin model shows a strong conformation to experimental data judging on satisfactorily values of the obtained linear regression coefficient, R^2 and non-linear error analyses table (3).

According to D-R isotherm the values of K_D less than unity imply adsorbents to consist of fine micropores and indicate a surface heterogeneity may be arisen from the pores structure as well as adsorbate-adsorbent interaction [28]. However, the model is quite able to describe the experimental data properly because of the goodness linear correlation and low SSE table (3).

3.7 Error analysis
The values of error analysis for Langmuir, Freundlich, Temkin and D-R isotherm models at 303K are presented in table 3. Apparently, it can be concluded that the most applicable isotherm to describe DBSA–materials adsorption system are Langmuir, and D-R isotherms. The values of regression coefficients, R^2 and the non-linear error functions SSE are in agreement to one another.

$$SSE = \frac{\sqrt{\left(q_{e,\exp} - q_{e,the}\right)^2}}{N} \tag{7}$$

where $q_{e,the}$ is the amount of sorbate adsorbed at equilibrium calculated from the model (mg.g^{-1}), $q_{e,exp}$ is the equilibrium value obtained from experiment (mg.g^{-1}) and N is the number of data points.

The linear regression coefficients R^2 are all more than 0.9, the resulted non linear regression analysis justified otherwise. Thus, Langmuir and DR isotherms are still significant to describe this adsorption system. Even though the linear regression coefficients, R^2 of the Temkin and freundlich are high than 0.9, these isotherms still the least applicable as the SSE are higher in value. The SSE value more than 5% is not recommended due to intolerant margin of deviation between the experimental data and the model calculated data.

3.8. Adsorption kinetics
Adsorption is a physiochemical process that involves the mass transfer of a solute (adsorbate) from the fluid phase to the adsorbent surface. A study of kinetics of adsorption is desirable as it provides information about the mechanism of adsorption, which is important for efficiency of the process. The applicability of the pseudo-first-order and pseudo-second-order model was tested for the adsorption of DBSA onto GeoM particles. The best-fit model was selected based on the linear regression correlation coefficient, R^2, values.

3.8.1. The first-order kinetic model
The Lagergren rate equation is one of the most widely used adsorption rate equations for the adsorption of solute from a liquid solution. The pseudo-first-order kinetic model of Lagergren may be represented by [29]:

$$\frac{dq_t}{dt} = k_1\left(q_e - q_t\right) \tag{8}$$

Integrating this equation for the boundary conditions t = 0 to t = t and q=0 to q = q_t, gives:

$$\ln\left(q_e - q_t\right) = \ln q_e - k_1 t \tag{9}$$

where q_e and q_t are the amounts of DBSA adsorbed (mg.g^{-1}) at equilibrium and at time t (min), respectively, and k_1 is the rate constant of pseudo-first-order adsorption (min^{-1}). The validity of the model can be checked by linearized plot of $\ln(q_e - q_t)$ versus t. The rate constant of pseudo-first-order adsorption is determined from the slope of the plot. The values of k_1 and q_e at different temperatures are presented in table (4).

3.8.2. The second-order kinetic model
The second-order kinetic model is expressed as:

$$\frac{dq_t}{dt} = k_2(q_e - q_t)^2 \tag{10}$$

Rearranging the variable in equation (10) gives:

$$\frac{dq_t}{(q_e - q_t)^2} = k_2 dt \tag{11}$$

Taking into account, the boundary conditions t=0 to t=t and q=0 to q=q_t, the integrated linear form of equation (11) can be arranged to obtain equation (12):

$$\frac{t}{q_t} = \frac{1}{k_2 q_e^2} + \frac{t}{q_e} \tag{12}$$

where q_e the equilibrium adsorption capacity and k_2 the second-order constant (g.mol^{-1}.min^{-1}) can be determined experimentally from slope and intercept of plot t/q_t versus t [30].

As discussed above, the validity of the model of Lagergren and the pseudo-second-order kinetic model can be checked by each linearized plot. If the second-order kinetics is applicable, then the plot of t/q_t versus t should show a linear relationship. The linear plots of t/qt versus t show good agreement between experimental ($q_{e(exp)}$) and calculated ($q_{e(cal)}$) values (Table 4). The correlation coefficients for the second-order kinetics model (R^2) are greater than 0.999, indicating the applicability of this kinetic equation and the second-order nature of the adsorption process of DBSA onto GeoM.

Table 4: Kinetic data calculated for adsorption of DBSA on GeoM

| Parameters		Kinetic models					
		Pseudo-first-order model			Pseudo-second-order model		
T(°C)	$q_{e(exp)}$ (mg.g^{-1})	$q_{e(cal)}$ (mg.g^{-1})	k_1 x10^3 (min^{-1})	R^2	$q_{e(cal)}$ (mg.g^{-1})	k_2 x10^3 (g.mg^{-1}.min^{-1})	R^2
35	977.7	1605.99	8.86	0.9378	980.39	2.43	0.9999
55	958	1484.75	7.56	0.9644	961.54	0.78	0.9999
65	928	1421.97	7.13	0.9771	925.92	2.72	0.9999
75	907.69	1398.17	6.83	0.9825	900.9	0.77	0.9999

3.9. Activation parameters
The activation energy of DBSA adsorption onto the GeoM can be calculated by Arrhenius relationship [31]:

$$\ln k_2 = \ln k_O - \frac{E_a}{R_g T} \tag{13}$$

where k_2 is the pseudo-second-order constant (g.mol^{-1}.min^{-1}), k_0 is the rate constant of adsorption (g.mol^{-1}.min^{-1}), E_a is activation energy of adsorption (J.mol^{-1}), R_g is the gas constant (8.314J.mol^{-1}.K^{-1}), T is the solution temperature (K). Plotting of ln k_2 against the reciprocal temperature gives a reasonably straight line, the gradient of which is $-E_a/R_g$. From equation (13), the activation energy, E_a, is 8.03 kJ mol^{-1}. The magnitude of activation energy gives an idea about the type of adsorption which is mainly physical or chemical. Low activation energies (5–50 kJ.mol^{-1}) are characteristics for physical adsorption, while higher activation energies

(60–800 kJ.mol^{-1}) suggest chemical adsorption [32]. This is because the temperature dependence of the pore diffusivity is relatively weak. Here, the diffusion process refers to the movement of the solute to an external surface of adsorbent and not diffusivity of material along micropore wall surfaces in a particle. The result obtained for the adsorption of DBSA onto GeoM indicates that the adsorption process is a physisorption (Figure 9). Therefore, the affinity of DBSA for GeoM may be ascribed to Van der Waals forces and electrostatic attractions between the DBSA and the surface of the particles. This low value of E_a generally indicates diffusion controlled process and higher values represent chemical reaction process. We can therefore conclude that the E_a value calculated from data suggest a diffusion-controlled process, which is a physical step in the adsorption process.
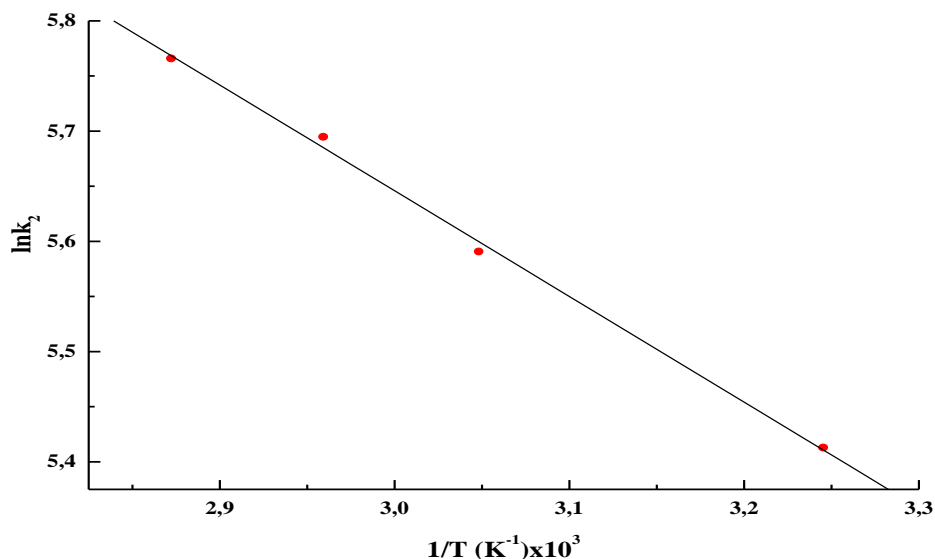
Figure 9. Arrhenius plot for the adsorption of DBSA on GeoM, μ=500 rpm, C_i=2.2 mMol.L^{-1}, pH= 4.5, m= 0.3g.

To calculate the activation parameters such as enthalpy (ΔH^*), entropy (ΔS^*) and free energy (ΔG^*), the Eyring equation was applied [33-34]:

$$\ln\left(\frac{k_2}{T}\right) = \ln\left(\frac{k_B}{h_P}\right) + \frac{\Delta S^*}{R_g} - \frac{\Delta H^*}{R_g T} \qquad (14)$$

where k_B is the Boltzmann constant (1.3807×10^{-23} J.K^{-1}), h_P is the Planck constant (6.6261×10^{-34} J.s), k_2 is the pseudo-second-order constant. Figure 10 has shown the plot of ln(k_2/T) against 1/T.
Gibbs energy of activation may be written in terms of entropy and enthalpy of activation:

$$\Delta G^* = \Delta H^* - T\Delta S^* \qquad (15)$$

The table 5 shows the corresponding values of activation Gibbs energy at different temperatures. The positive ΔG^* value suggests that adsorption reactions require energy to convert reactants into products. The ΔG^* value determines the rate of the reaction, rate increases as ΔG^* decreases, and hence the energy requirement is fulfilled, the reaction proceeds. The positive value of ΔH^* (5.28 kJ.mol^{-1}) confirms the endothermic process, meaning the reaction consume energy. The negative value of ΔS^* (-180 J.K^{-1}.mol^{-1}) indicates that the

adsorption leads to order through the formation of activated complex suggesting that DBSA adsorption on GeoM surface is an associated mechanism. Also the negative value of ΔS^* normally reflects that no significant change occurs in the internal structure of the adsorbent during the adsorption process [35].
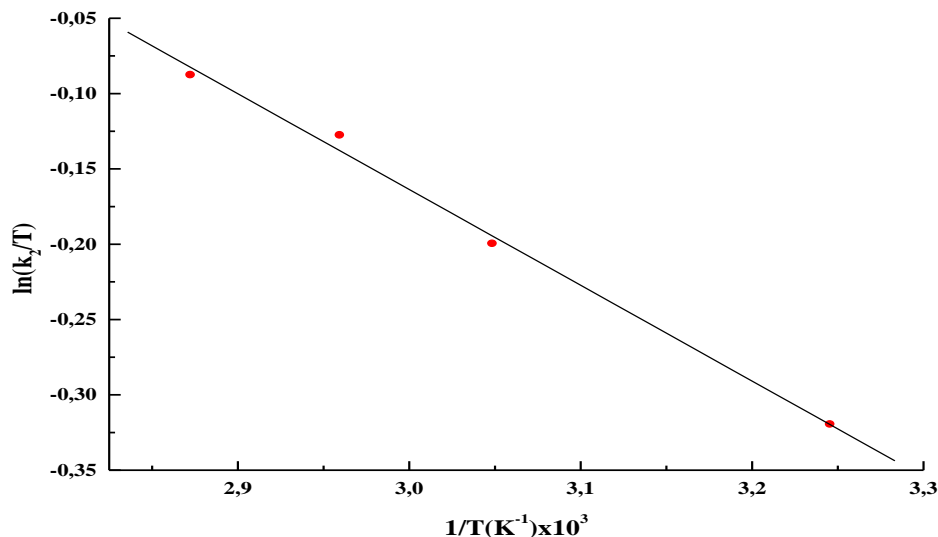
Figure 10. Plot of $\ln(k_2/T)$ versus $1/T$ for adsorption of DBSA on GeoM, μ=500 rpm, C_i=2.2 mMol.L^{-1}, T= 25°C, pH= 4.5, m= 0.3g.

Table 5: Thermodynamic properties of DBSA-GeoM adsorption system

	GeoM			
ΔH^* (kJ.mol^{-1})	5,28			
ΔS^* (J.K.mol^{-1})	-180			
Ea (kJ.mol^{-1})	8.03			
T (K)	308	328	338	348
ΔG^* (kJ.mol^{-1})	61,66	65,32	67,15	68,98

Conclusion

The adsorption potential of geomaterial developed from natural materials for the dodecylbenzene sulfonic acid pollutant was evaluated. The sorbent properties of the new material relative to the individual components were compared; the comparison should have been established by the performing sorption and kinetic experiments. The results indicate that the removal of dodecylbenzene sulfonic acid by geom was primarily attributed to the potential sorbent of the inorganic part of geomaterial. The results show that 0.3 g of geomaterial was at least as effective for LAS removal as 7- or 10- fold larger concentrations of activated carbon and montmorillonite, respectively. The interest of this study lies whether the new material has more promising sorbent properties than the individual components. Otherwise the results show that CMC parameter plays a determinant role because there was no further adsorption beyond the CMC value and that adsorption was favorably influenced by decreased pH, increased temperature and low initial concentration. The Thermodynamic values of (ΔG^*, ΔH^*, ΔS^*) indicate the adsorption of dodecylbenzene sulfonic acid on the geomaterial surface is endothermic not spontaneous in nature and leads to order by the formation of activated complex, suggesting to a mechanism associated.

References

1. Marcomini, A., Giger, W. Tenside Surfactants Detergents. 25 (1988) 226-229.
2. Odokuma, L.O., Okpokwasili, G. C. Environmental Monitoring Assessment. 45 1 (1997) 43- 57.
3. Fable, J. Surfactant in consumer products: theory, technology and application, Springer, (1986).
4. Lin, S. H., Lin, C. M., Leu, H. G. Water Research. 33 7 (1999) 1735-1741.
5. Rozzi, A., Antonelli, M., Angeretti, C. Journal of the society of leather technologists and   chemists. 84 6 (2000) 266-270.
6. Wu, S. H., Pendleton, P. Journal of Colloid and Interface Science. 243 2 (2001) 306-315.
7. Prats, D., Ruiz, F., Vazquez, B. Water Research. 31 8 (1997) 1925-1930.
8. Zhang, M., Liao, X., Pin, S. Journal of the society of leather technologists and chemists. 90 (2005)   1-6.
9. Pavan, P.C., Crepaldi, E. L., Valim, J. B. Journal of Colloid and Interface Science. 229 2   (2000) 346-352.
10. Vanjara, A. K., Dixit, S. G. Langmuir. 11 7 (1995) 2504.
11. Brown, W., Zhao, J. X. Macromolecules. 26 11 (1993) 2711-2715.
12. Gupta, S., Pal, A., Gosh, P. K, Bandyopadhyay, M. Journal of Environmental Science and   Health Part A: Toxic/Hazardous Substance and Environmental Engineering. 38 2 (2003) 381-397.
13. Hamdi, B., Houari, M., Ait hamoudi, S., Kessaissia, Z. Desalination.166 (2004) 449-455.
14. Cserhati, T., Forgacs, E., Oros, G. Environment International. 28 5 (2002) 337-348.
15. Sennour, R., Mimane, G., Benghalem, A., Taleb, S., Applied Clay Science. 43 3-4 (2009) 503-506.
16. Jover, A., Meijide, F., Mosquera, V., Vázquez, Tato. Journal of Chemical Education. 67 (1990) 530.
17. Shukla, A., Zhang, Y.H., Dubey, P. Journal of hazardous Materials. 951-2 (2002) 137-152.
18. Gordon, M. Use of adsorbents of pollutants from wastewaters, CRC Press, New York. (1996)
 59-65.
19. Vemulapalli, G.K. Physical Chemistry, Prentice Hall: Englewood Cliffs, NJ, (1993).
20. Rodriguez-Prieto, M. F., Rios-Rodriguez, M. C., Mosquera-Gonzalez, M., Rios-Rodriguez, A. M., Mejuto-Fernandez, J. C. Journal of Chemical Education. 72 7 (1995) 662-663.
21. Schouten, N., Ham Van Der, L.G.J., Euverink, G.J.W., Haan De, A.B. Water Research. 41 (2007) 4233-4241.
22. Langmuir, I. Journal of American Chemical Society. 40 (1916) 1361-1368.
23. Freundlich, H. M. F. Journal of physical Chemistry. 57 (1906) 385-470;
24. Aharoni, C., Ungarish, M. Journal of the Chemical Society Faraday Transactions.73 (1977) 456-464.
25. Dubinin, M. M. Chemical Reviews. 60 (1960) 235-266.
26. Hassany, S. M., Chaudhary, M. H. Applied Radiation and Isotopes. 47 (1996) 467-471.
27. Mal, I.D., Srivastava, V.C., Agarwal, N.K. Dyes and Pigments. 69 3 (2006) 210-223.
28. Kim, B.T., Lee, H.K.,Moon, H.,Lee, K.J. Separation and Purification Technology. 30 16 (1995) 3165-3182.
29. Lagergren, S. Zur theorie der sogenannten adsorption geloster stoffe. Kungliga Svenska Vetenskapsakademiens, Handlingar. Band. 24 4 (1898) 1-39.
30. Ho, Y. S., McKay, G. Journal of Chemical Engineering. 76 4 (1998) 822-827.
31. Thomas, W.J., Crittenden, B. Adsorption Technology and Design. Reed Educational and Professional Publishing, Oxford. (1998) 27-32-68.
32. Nollet, H., Roels, M., Lutgen, P., Van Der Meeren, P., Verstraete, W. Chemosphere. 53 (2003) 655-665.
33. Eyring, H. Journal of Chemical Physics. 3 (1935) 107-114.
34. Laidler, K.J., Meiser, J.M. Physical Chemistry, Houghton Mufflin, New York. (1999) 852.
35. Anirudhan,T.S., Radhakrishnan,P.G.The Journal of Chemical Thermodynamics.40 (2008) 702-709

(2012) www.jmaterenvironsci.com